Composition of mortar as a function of distance to the brick-mortar interface: a study on the formation of cured mortar structure in masonry using NMR, PFM and XRD

H.J.P. Brocken and J.A. Larbi
TNO Building and Construction Research, Division of Building Technology
P.O. Box 49, NL-2600 AA Delft, The Netherlands

L. Pel
Eindhoven University of Technology, Faculty of Applied Physics
P.O. Box 513, NL-5600 MB Eindhoven, The Netherlands

N.M. van der Pers
Delft University of Technology, Faculty of Applied Sciences
P.O. Box 5, NL-2600 AA Delft, The Netherlands

The formation of cured mortar structure in masonry was studied using multiple experimental techniques. Starting with fresh mortar, nuclear magnetic resonance (NMR) was used to measure the water extraction during brick laying. After curing, the composition of cured mortar was investigated with polarizing and fluorescent microscopy (PFM) and X-Ray diffraction (XRD).

Two typical mortars were investigated: a cement-lime mortar and a cement mortar with air entraining agent. The measurements indicate that the mortar composition (i.e. the contents of sand, cured binder and voids) and the contents of chemical substances of the cured binder (i.e. the contents of calcite and portlandite) change with distance to the brick-mortar interface. For the cement mortar with air entraining agent, the observations are explained by the enrichment of binder towards the brick-mortar interface, resulting from the local compaction and compression of the fresh mortar. In the cement-lime mortar such an enrichment of binder hardly occurs and the observations are explained by the intense carbonation that takes place. As a result, the chemical composition of the binders is very much different in both mortars. In the cement mortar with air entraining agent, near the brick-mortar interface the enrichment of cement and the low water content (resulting from the low water retentivity of this mortar), lower the water-to-cement ratio and as a consequence the cement is not fully hydrated. In the cement-lime mortar, because the $Ca(OH)_2$ content and the water content is higher, near the brick-mortar interface, a carbonated zone is formed which is hardly permeable for CO_2 (and probably water). The latter does not occur in the cement mortar, it remains permeable.

HERON, Vol. 44, No. 4 (1999) ISSN 0046-7316

The analysis of the experimental results have lead to the formulation of a conceptual model for the formation of cured mortar structure in masonry. Such a model may be helpful in analysing and predicting the durability of mortars.

Keywords: **masonry, mortar characteristics, mortar composition, moisture transport, curing & carbonation**

1 Introduction

Properties like the brick-mortar bond, the mortar permeability, its strength and stiffness and the leaching of mortar are important characteristics that determine the durability and service life of mortar joints and masonry. These properties are influenced by a number of parameters. Firstly, of fresh mortar the contents of binder (cement and / or lime), sand, other chemically inactive components (limestone), and water as well as the grain size distribution of the sand are important. Secondly, the water extraction from the fresh mortar during brick laying is of great influence. This water extraction strongly influences the curing of the mortar. The water extraction is determined by the sorption characteristics of the brick and the so-called water retentivity of the fresh mortar. Altogether, the numerous parameters involved, complicate a distinct prediction and classification of mortar durability.

In the past, cement-lime mortars were more applied in masonry than cement mortars. However, after the introduction of air entraining agents which increase the workability of mortar, the cement mortars have become more popular because their curing proceeds much faster than the curing of cement-lime mortars. With respect to the cement-lime mortars it is observed that mortar joints are almost impermeable to water [1], while for cement mortars with air entraining agent it is observed that the strength of the brick-mortar bond decreases with increasing amounts of air entraining agent [2]. Because of these typical characteristics, the composition of both mortar types was studied as a function of distance to the brick-mortar interface.

The water extraction from the fresh mortar by the brick was measured using Nuclear Magnetic Resonance (NMR). The composition of the mortars, that is the porosity (air-voids content), contents of sand and hardened binder and the mineralogical composition of the hardened binder were analysed using polarizing and fluorescent microscopy (PFM) and X-Ray diffraction (XRD). The results obtained from these specialised measuring techniques are used to formulate a more general model for the formation of cured mortar structure in masonry. Such a model is useful in predicting and explaining the characteristics of mortar joint and brick-mortar bond.

2 Mortar and masonry characteristics

In the present paper, the investigated cement-lime mortar and cement mortar with an air entraining agent are indicated as LCM and PCM_{aea}, respectively. An overview of the constituents of the fresh mortars is given in Table 1.

For the preparation of small masonry segments to be used in the analyses, four machine moulded red fired-clay bricks and either mortar LCM or mortar PCM_{aea} were used. Since in this study the

characteristics of the interface of brick and mortar were very important, it was necessary to prepare these interfaces in a reproducible manner. Especially the sanded sides of the brick resulting from the sanding of moulds, could evoke irregularities of the interface and its characteristics. Therefore it was chosen to remove a thin top layer of 1–2 mm from the bricks by slicing. As a result, flat brick surfaces were obtained. The bricks were applied dry in the masonry segments. The corresponding sorptivity, S, for initially dry brick was 0.42 $kgm^{-2}s^{-0.5}$. Additional characteristics of this type of brick are given in [1]. Each masonry segment consisted of 4 bricks with about 12 mm thick mortar layers in between. After brick laying, the masonry segments were cured for one day under damp cloths and thereafter for a period of at least 28 days at 20°C and a relative humidity of 50%.

3 Water extraction from fresh mortar during brick laying

The water extraction was measured using Nuclear Magnetic Resonance (NMR) [3]. In such a NMR experiment, the magnetic moments of the hydrogen nuclei are manipulated by suitably chosen alternating radio frequency fields, resulting in a so-called spin-echo signal. The amplitude of this spin-echo signal is proportional to the amount of hydrogen nuclei excited by the radio frequency field. The resonance condition for the nuclei is given by $f = \gamma/2\, B_0$. Here, f is the frequency of the alternating field, γ is the gyromagnetic ratio of the nuclei ($\gamma/2 = 42.58$ MHz / T for ^1H), and B_0 is the magnitude of the externally applied static magnetic field. Because of the resonance condition, the method can be made sensitive to only hydrogen and therefore to water. When a known magnetic field gradient is applied, the resonance condition will depend on the spatial position of the nuclei. By varying the frequency f, the moisture distribution can be measured without moving the sample.

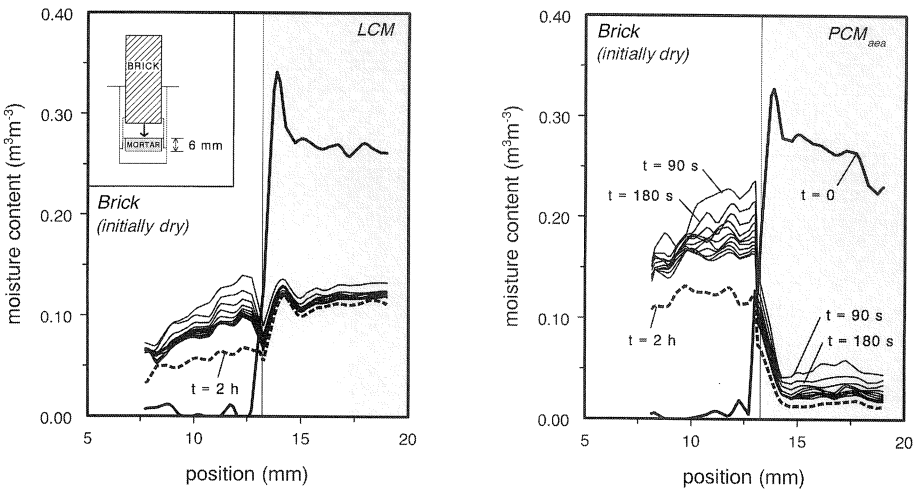

Fig. 1. Moisture profiles measured during water extraction from (a) mortar LCM *and (b) mortar* PCM_{aea}. *The bold curves show the initial moisture profile in the brick and the mortar. In both figures, the first 10 profiles measured every 90 seconds, together with the last measured profile (the dashed curve) are given. The shaded areas represent the mortar layers.*

In the experimental set-up (see inset in Figure 1), a cylindrical brick sample of 20 mm diameter and 50 mm length was placed upon a 6 mm thick layer (half of the thickness of the used mortar joint) of fresh mortar at the bottom of a cylindrical teflon holder (internal diameter of 20 mm). Each 90 s a moisture content profile (that is, moisture content as a function of position) was measured in the brick and the mortar, starting immediately after the brick was placed on top of the fresh mortar. An extensive description of the water extraction is given in [4].

Table 1. The constituents and amounts used for the preparation of mortar LCM, mortar PCM_{aea} and mortar PCM. Mortar LCM contains lime ($Ca(OH)_2$) whereas mortar PCM_{aea} contains air entraining agent (aea).

		sand	cement	lime	aea	water
LCM	Rel. Mass	5.6	1	0.27	-	1.2
	Rel. Volume	4.5	1	0.70	-	1.5
PCM_{aea}	Rel. Mass	5.6	1	-	$3{\cdot}10^{-5}$	1.2
	Rel. Volume	4.5	1	-		1.4
PCM	Rel. Mass	5.6	1	-	-	1.2
	Rel. Volume	4.5	1	-	-	1.6

Table 2. Survey of the moisture contents (m^3m^{-3}) and the water-to-cement ratios (mass%) "in the middle" of the fresh mortars, before and after the water extraction. The initial water-to-cement ratio is copied from Table 1. The remaining water-to-cement ratio (printed in italics) is estimated from its initial value using the ratio that is indicated by the initial and remaining moisture contents.

	Moisture content			Water-to-cement ratio	
	initial	remaining	extracted	initial	*remaining*
LCM	0.27	0.11	0.15	1.5	*0.5*
PCM_{aea}	0.26	0.02	0.24	1.4	*0.1*
PCM	0.25	0.04	0.21	1.6	*0.2*

NMR Results

In Figure 1 for mortar LCM and PCM_{aea}, the measured moisture profiles during water extraction are presented. As can be seen, most of the water is extracted out of the mortar within the first 90 seconds. The same phenomenon was observed for other mortars. (Note that the water extraction rate is determined primarily by the sorption characteristics of the brick [1, 4].) However the water that remains in the mortar after reaching equilibrium, strongly depends on the mortar type. For mortars LCM, PCM_{aea} and PCM (a cement mortar without an air entraining agent) these amounts, representing the moisture content in "the middle" of the mortar joint, are summarized in Table 2. As can be seen

from Table 2 and Figure 1, in the case of mortar LCM the remaining moisture content is about 5 times higher than in the case of mortar PCM_{aea} and 2.5 times higher than in the case of mortar PCM. Thus mortar LCM retains more water for its curing while mortar PCM_{aea} retains just a very small amount of water. The remaining moisture contents roughly correspond with water-to-cement ratios of about 0.5, 0.1 and 0.2 (by mass) for mortar LCM, mortar PCM_{aea} and mortar PCM.

4 Composition of cured mortar as a function of position

4.1 *Polarizing and fluorescent microscopy (PFM)*

Polarizing microscopy enables the determination of the various components including the air-void content of mortar. In this technique a beam of light entering an anisotropic crystal (which is optically birefringent), splits into two beams of polarized light with different indices of refraction. As a consequence, when viewed in a microscope between crossed polars [5], such crystals cause some light to pass through. When the thickness of the sample is below 30 μm, the characteristic interference colours and other optical properties of the various minerals in the mortar can be used to identify each of the constituents present. Moreover, in plane polarized light, voids that are impregnated with a fluorescent resin will show their characteristic fluorescent colour. By means of a simple point counting process, the void content, the binder content and the sand content can be determined [6]. For a thin section of concrete, with a section area of 100 mm x 50 mm or larger, the inaccuracy of such a point counting process is less than 2% [7]. For mortar samples, which generally contain smaller sand particles, the inaccuracy is expected to be better than for concrete.
The optical microscopy was performed with a Zeiss Axioplan microscope using a 12V / 100W halogen source.

Sample Preparation

For the microscopical analysis, small blocks were sawn from the masonry. These small blocks were impregnated with an epoxy resin containing a fluorescent dye. One surface of such an impregnated block was polished and glued to an object glass. A thin slice for microscopy was then prepared as follows. First the object glass together with a thin material layer was detached from the block by sawing. After that, the thin layer that remained on the object glass was ground and polished until a slice of 20-30 μm thickness was left on the object glass. The area of this slice was approximately 50 mm x 30 mm.

Microscopy Results

The contents of sand, cured binder and voids of mortars LCM and PCM_{aea} are plotted in Figure 2 as a function of distance to the brick-mortar interface. In the middle of the mortar joint, for both mortars the sand content is the same, whereas in mortar PCM_{aea} the hardened binder content is about 20% lower (and the void content is about 25% higher) than in mortar LCM. Towards the brick-mortar interface the sand content increases and then clearly decreases near the interface. In mortar PCM_{aea} the decrease of the sand content near the brick-mortar interface is much larger than in mortar LCM. In both mortars the hardened binder content increases towards the brick-mortar interface. In mortar PCM_{aea} this increase is larger and is observed in a wider zone than in mortar LCM. The trend of the

void content is opposite to the trend of the sand content; near the brick-mortar interface, the void content first decreases and then increases at this interface. For both mortars the decrease as well as the increase of the void content is more or less the same. For mortar PCM_{aea} the void content is about 15% higher than for mortar LCM.

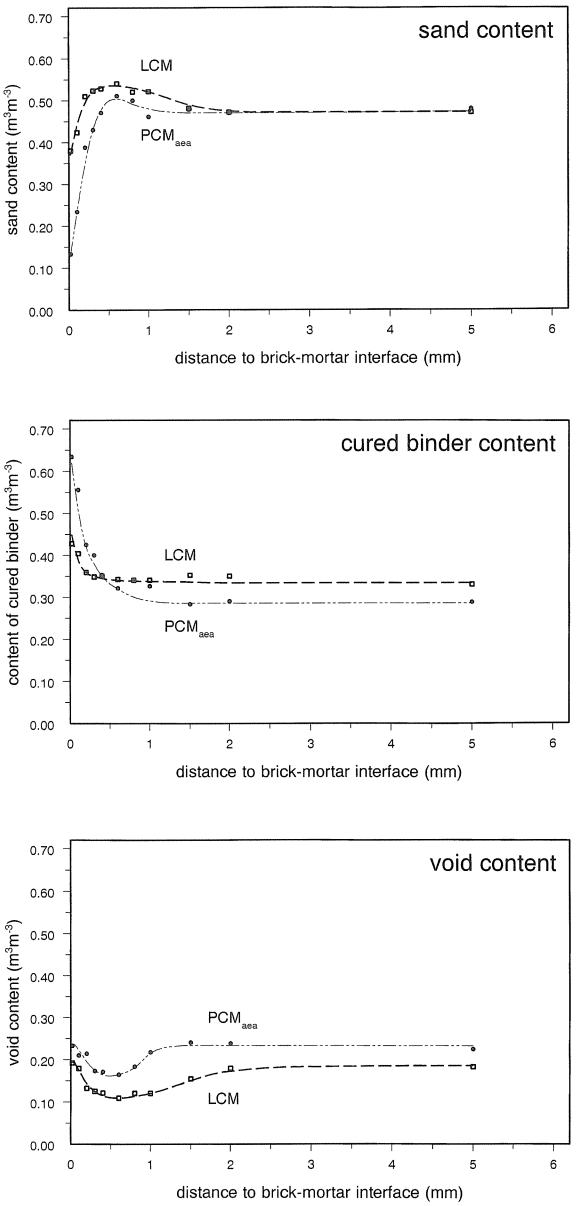

Fig. 2. The (a) sand, (b) cured binder and (c) void content of mortar LCM (□) *and mortar* PCM_{aea} (●) *as a function of distance to the brick-mortar interface.*

For mortar LCM and mortar PCM_{aea} the composition is presented in Figure 3. It is observed that in mortar LCM carbonation occurs up to 1.0 mm from the brick-mortar interface[1], whereas in mortar PCM_{aea} carbonation occurs more or less homogeneously throughout the whole mortar joint. In mortar LCM, carbonation is found throughout the cement paste islands (in the 1 mm zone), whereas in mortar PCM_{aea} carbonation is found only at the surface of cement paste islands that are in contact with voids.

In mortar LCM, clusters of lime (mainly $Ca(OH)_2$) were only identified in the cement paste islands that are outside the carbonated zone; in mortar PCM_{aea} no $Ca(OH)_2$ was found.

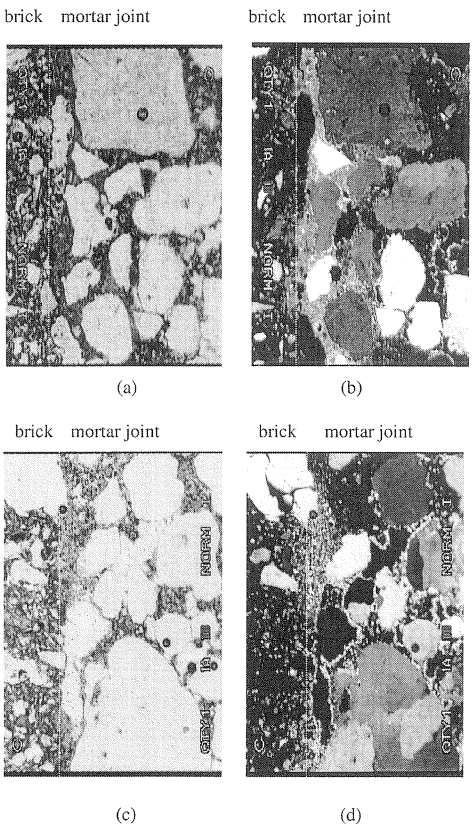

Fig. 3. Micrographs of the brick-mortar interface of (a, b) mortar LCM *and (c, d) mortar* PCM_{aea}*; the micrographs are obtained with plane-polarised light and illustrate an area of 2.7 mm x 1.8 mm. To visualise calcite (i.e. carbonation), micrographs (b) and (d) are viewed through crossed polars. In these figures the brick-mortar interface is indicated by the dashed line. In the left-hand-side micrographs the sand particles are white, the void space is yellow and the cement paste is grey/ black.*

[1] In the left-hand-side micrograph of Figure 3 the composition of the mortars is visualised through plane polarised light. In the right-hand-side micrograph the same composition is viewed through crossed-polars so that calcium carbonate, the product of carbonation of lime (calcium hydroxide), lights up yellow.

4.2 *X-Ray diffraction analysis* (XRD)

X-Ray diffraction allows qualitative and semi-quantitative chemical analysis of polycrystalline materials to be made in terms of contents of crystalline phases [8], rather than in terms of content of chemical elements.

Qualitative analysis is accomplished by identification of the characteristic diffraction line pattern of each phase, which forms a sort of fingerprint. A large number of known diffraction patterns is collected in the Powder Diffraction File (PDF) from the International Centre for Diffraction Data. This PDF file was used to identify the phases present in the cured mortars. Semi-quantitative analysis is based on the fact that the integrated intensity, of each diffraction line of a particular phase in a mixture of phases, correlates with the content of that phase in the mixture. The integrated intensity is in general not directly proportional to the content, because the intensity depends (*i*) on the (effective) X-Ray absorption coefficient of the mixture, which in itself varies with chemical composition and (ii) on the way in which the crystallites are oriented in the sample. Although in the present investigation the content of the phases in the mortars varies, the absorption coefficient was constant due to the fact that the bulk chemical composition is the same throughout the mortar. To check the orientation distribution of the crystallites in the mortar, the ratios of the intensities of the measured diffraction lines of each phase were monitored. It was found that this orientation distribution did not change in the mortar so that fractional changes in the integrated intensity of each diffraction line were equal to fractional changes in the content of the phase concerned.

The measurements were performed on a Siemens D500 diffractometer equipped with a diffracted-beam graphite monochromator (CuKα-radiation). More information on the measured diffraction angles and the analysed reflections is given in [9].

Sample Preparation

For X-Ray diffraction analysis, masonry cylinders of 45 mm diameter with 2–3 mm thick brick layers at the ends and 12 mm mortar layer in the middle were drilled from the masonry segments. These cylinders were impregnated with an epoxy resin. After that, at one end of the cylinders, the brick layer was gently removed by grinding. Once the mortar surface was reached (that is, the brick-mortar interface), a flat sample surface was obtained by polishing. The flatness of the surface and its parallelism with the brick-mortar interface was controlled to within 20 μm by thickness measurements at 8 equidistant positions along the circumference of the polished surface. Within two days after polishing the samples were analysed. (It was established that the integrated intensities of the analysed reflections did not change during this period.) For analysing the mortar at positions away from the brick-mortar interface, the grinding and polishing procedure was repeated.

X-Ray Diffraction Results

The contents of calcite and portlandite found for the mortars LCM and PCM_{aea} are plotted in Figure 4 as a function of distance to the brick-mortar interface: clearly the contents of the studied substances strongly vary in a 2-3 mm thick mortar layer near to the brick-mortar interface.

For calcite (calcium carbonate: $CaCO_3$) the curves are very much different for the two mortars. For mortar LCM, the content of calcite at the brick-mortar interface is about three times higher than for mortar PCM_{aea}. Besides, for mortar LCM the content of calcite decreases strongly with the distance to

the brick-mortar interface, whereas for mortar PCM_{aea} first the content of calcite increases slightly and then, from about 0.5 mm, it remains unaltered.

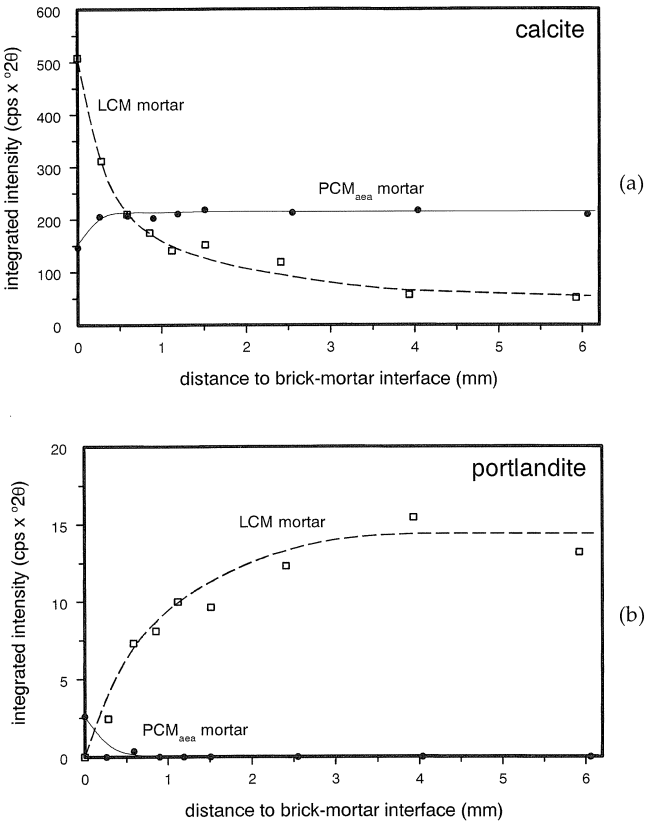

Fig. 4. The contents of (a) calcite and (b) portlandite determined for mortar LCM (□) *and mortar* PCM_{aea} (●) *as a function of distance to the brick-mortar interface. As a guide to the eye, the lines indicate the measured trend for each phase.*

For portlandite (calcium hydroxide or lime: $Ca(OH)_2$), the trends are reverse to the trends of calcite. The content of portlandite at the brick-mortar interface is zero for mortar LCM and for mortar PCM_{aea} relatively small (roughly five times smaller than that in the middle of mortar joint LCM). Furthermore, for mortar LCM the content of portlandite increases with the distance to the brick-mortar interface, whereas for mortar PCM_{aea} the content of portlandite decreases sharply to zero. As with calcite, the effects for portlandite are much stronger in mortar LCM than in mortar PCM_{aea}. Especially for the interpretation of the results for mortar LCM, it is essential that CO_2 diffusion is prevented by impregnation of the mortar sample with a resin. If not, the measured trend for calcite showing an increase towards the brick-mortar interface, could be a result of CO_2 diffusion after the sample preparation.

Therefore this was checked independently by repeating, after a considerable time, the X-Ray diffraction analysis for the middle of the mortar (that is, at about 6 mm from the brick-mortar interface) since here the conditions for carbonation are favourable (that is, a high portlandite content and a low calcite content occur). This additional analysis showed that in a time period of about 3 months no further carbonation had occurred. Obviously the measured trend of the calcite content represents a state of carbonation present at the moment the samples were impregnated.
In mortar LCM also some vaterite (another allotropic modification of calcium carbonate) was found. Although no quantitative analysis of vaterite was possible because of overlapping ettringite reflections, the changes in the intensities of the vaterite peaks strongly suggest that the decrease of the content of vaterite with distance to the brick-mortar interface is very similar to the decrease of the content of calcite (see Figure 4). In mortar PCM_{aea} some alite was found near to the brick-mortar interface only.

5 Discussion

The composition profiles as obtained by the microscopical (point counting) analysis, represent the amounts of sand, cured binder and voids. The trends of these profiles can be explained by differences in the water content (and water extraction) of the fresh mortar resulting in different degrees of compaction and compression[2]; see Figure 5. The composition profiles as obtained by the X-Ray diffraction analysis represent the chemical composition of the cured binder in terms of the diffracted intensity of the individual phases. For the explanation of the trends of the composition profiles, first the effect of water will be elucidated.

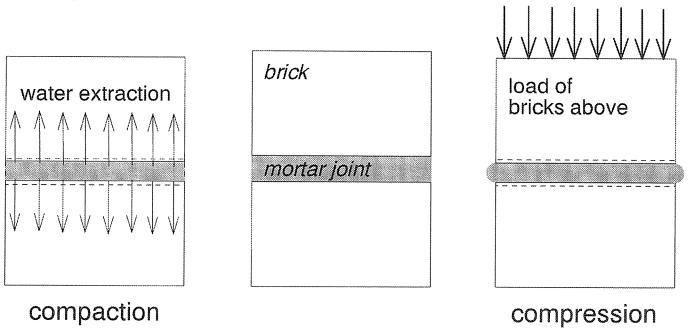

Fig. 5. Schematic presentation of compaction (overall increase of sand content) and compression (local increase of sand content near the brick-mortar interface) of mortar joints.

[2] Compaction in this particular case refers to the rearrangement of sand particles caused by the water extraction. This results in a denser mortar structure. Compaction is influenced by the water content and occurs on a homogeneous scale. Compression occurs during the plastic phase of fresh mortar and is caused by the weight of brick(s) above. It shows a decrease of volume on top of the mortar joint and an increase of volume at the sides (see Figure 5). The relatively large sand particles are not mobile and will not redistribute to the sides of the mortar joint. Compression therefore results in a local compaction of sand particles (an increase of the sand content and a decrease of the void content) near the brick-mortar interface.

Before brick laying, the fresh mortar contains sand, binder, air and water. The amount and behaviour of the water plays a dominant role from the moment of brick laying, until the final composition after curing. The behaviour of the water can be divided into three parts: i) filling the space between the sand particles, giving the fresh mortar its plasticity (workability); ii) it is extracted by the bricks, causing compaction of the fresh mortar structure (predominantly packing of the sand particles); iii) reacting with the binder, forming the cured binder material. In the cured mortar, after evaporation (drying) of the residual water, the volume of this water stays behind as (small) voids together with the original air voids.

The overall amounts of water are given in Table 2, showing that the amount of retained water is ca. 0.10 m^3m^{-3} for mortar LCM and ca. 0.02 m^3m^{-3} for mortar PCM_{aea}. NMR measurements show an almost flat moisture content profile over the whole mortar joint, except for a zone of ca. 0.5 mm from the bricks where no information is present due to the limited spatial resolution of 1 mm of the NMR equipment [3]. (Theoretically near the brick-mortar interface the moisture content must be lower than in the middle of the mortar joint.) If the amount of water is the same everywere, the above mentioned three processes will take place uniformly over the whole mortar joint. For "the middle part" of the joint up to a distance of ca. 2 mm from the bricks, this uniformity is indeed observed for each of the profiles in Figure 2. For that middle part, for both mortars the sand content is the same and the differences in cured binder and void contents are related to the amounts of the mortar constituents of the fresh mortar (see Table 1: the sand content is the same for both mortars; for mortar LCM the binder content is higher and the air content is lower than for mortar PCM_{aea}). Taken the sand content as a measure for the degree of compaction, it follows from Figure 2a that for the middle part of the joint the relatively large differences in amount of retained water of both mortars did not result in different degrees of compaction in the cured mortars.

The increase of the sand content starting from ca. 2 mm near the bricks can be explained by the fact that due to the load of the bricks the compression will increase towards the brick surface. This effect is clearly indicated by the decrease of the void content in this region (Figure 2c). The compression is larger for mortar LCM than for mortar PCM_{aea}; it seems that in this region the high amount of retained water for mortar LCM favours the compression.

The subsequently steep decrease in the sand content starting from ca. 0.5 mm towards the bricks, is explained by the combination of a (theoretical) decrease of the water content, and the so-called "wall-effect" [10]. A theoretical decrease of the water content near the brick-mortar interface (not actually measured with NMR) results in a poorer local compaction of the sand particles (i.e. a decrease of the sand content). By that it can be explained that in mortar LCM, presumed to have a higher water content near the brick-mortar interface than mortar PCM_{aea}, the local compaction is better (i.e. the local sand content is higher) than in mortar PCM_{aea}; analogous to compaction of concrete [11]. The wall-effect is a pure geometrical phenomenon resulting in more space between the sand particles (a lower concentration). The zone in which this effect will strongly counteract the increase due to the compression will be about half the size of the largest sand particles (i.e. ca. 0.5 mm).

The above reasoning is set up, bearing in mind the sand as it has the highest volumetric portion in the mortar. The sand particles are also the largest particles present in the mortar and as a consequence packing of the mortar structure starts with the packing of sand particles. Binder particles are much smaller and, with some water, remain plastic (and mobile) during the first stages of packing and curing of the mortar. Therefore the observed cured binder content (Figure 2b) is considered to result primarily from filling up the open space between the sand particles. As a secondary effect this cured binder content may also be increased by transport of binder with the water flow from fresh mortar to brick. In mortar LCM, having a denser structure and retaining more water than mortar PCM_{aea}, binder transport may be neglected. In mortar PCM_{aea}, binder transport may have had a contribution to the enrichment of binder near the brickmortar interface.

The explanation of the composition profiles is complicated; not only the enrichment of binder near the brick-mortar interface plays a role but also the different compositions of the fresh mortar (see Table 1) and the related curing and carbonation reactions.

The calcite and portlandite content profiles are closely related because the calcite originates from the portlandite through carbonation. The degree of carbonation in the binder strongly depends among others, on the presence of CO_2 and on the contents of water and $Ca(OH)_2$. The higher the contents the more calcite is formed. However, as a result of different curing and carbonation, the occurrence of portlandite and calcite originating from it is quite different in mortars LCM and PCM_{aea}. In mortar LCM, the $Ca(OH)_2$ (portlandite) is available by the addition of lime (mainly $Ca(OH)_2$) and after the cement hydration, whereas in mortar PCM_{aea} the $Ca(OH)_2$ is only available after the cement hydration. As in mortar LCM also the water content is higher than in mortar PCM_{aea} (see Table 2), the highest degree of carbonation is expected in mortar LCM. This is indeed observed, see Figure 4. Remarkably, this figure also indicates that in the case of mortar LCM not the whole mortar joint is carbonated but only a zone near the brick-mortar interface. Apparently CO_2 is supplied by diffusion by the brick, thereby creating the so-called carbonated zone. In this zone carbonation has occurred throughout the cement paste islands (see the microscopical analysis). It is well known that as a result of intense carbonation, the microstructure of ordinary portland cement gets denser [10]. Apparently through the carbonated zone in mortar LCM, CO_2 penetration is hindered and as a result, outside the carbonated zone little carbonation is observed: a relatively high portlandite content and a low calcite content occur (see Figure 4).
In mortar PCM_{aea} the carbonation conditions are much different. The water content is about 5 times lower than in mortar LCM (see Table 2 and Figure 1) and $Ca(OH)_2$ only becomes available from the cement hydration. In this mortar, CO_2 is also supplied by diffusion by the brick. However, due to the lower water content of this mortar, there is less CO_2 dissolved in the cement paste islands than in the case of mortar LCM. Thus less carbonation can occur in the cement paste islands. Moreover, in ordinary cement paste $Ca(OH)_2$ precipitates out of the pore solution forming crystals, preferably on the sand particles [12]. Consequently at the boundary of the cement paste islands the concentration of $Ca(OH)_2$ will have increased and carbonation will occur primarily on sand particles and at the boundary of cement paste islands. Such a typical carbonation is confirmed by the microscopical observations; in mortar PCM_{aea} carbonation occurs at the boundaries of the cement paste islands and not much inside them. Carbonation is observed by the same extent everywhere in mortar PCM_{aea} (see

Figure 4), which indicates that CO_2 penetration is not noticeably hindered by the carbonation, as in mortar LCM. Furthermore the portlandite content is approximately zero throughout mortar PCM_{aea} (see Figure 4). To explain this, the above supposition that $Ca(OH)_2$ precipitates out of the pore solution of the cement paste islands [12] is essential. After full hydration of the cement (no alite was found in the middle of mortar PCM_{aea}), dissolved $Ca(OH)_2$ diffuses towards the boundary of the cement paste islands where it can be carbonated. As a consequence the portlandite content is zero inside as well as at the boundary of the cement paste islands.
Apparently, at the brickmortar interface in mortar PCM_{aea} the carbonation conditions differ from the middle of the mortar since there the calcite and portlandite contents deviate (see Figure 4). At the interface alite (C_3S) is observed, indicating that not all the cement is hydrated. Obviously towards this interface the cement content was increased so much and the water content was so low (see the explanation above for the poor local compaction at the brick-mortar interface in mortar PCM_{aea}) that the available water has not been sufficient for full cement hydration. By this shortage of water, the $Ca(OH)_2$ in the cement paste islands can not fully dissolve and diffuse towards the boundary of the cement paste islands. Consequently not all $Ca(OH)_2$ can carbonate and at the brick-mortar interface the calcite content slightly decreases and the portlandite content increases (see Figure 4).

6. Conclusions

For cement-lime mortars, as a result of the high binder content and the high degree of carbonation, near the brick-mortar interface a carbonated zone is formed which delays seriously the penetration of CO_2 and most probably hinders the permeation of water. This provides an explanation for the experimental observations showing that in masonry with cement-lime mortar, capillary rise stops at the mortar joints.
In cement mortars with air entraining agent the water retentivity is low and as a result of enrichment of cement near the brick-mortar interface, at this interface the cement may not be fully hydrated as is observed in the present research. This may cause poor bonding of this mortar with the brick. Reasoning towards practical implications, such an effect condemns combinations of mortars with low water retentivity and bricks with high sorptivities.

In the conceptual model on the formation of mortar structure that is described in the discussion, the water content in a zone of 1 mm near the brick-mortar interface is very important. However, due to the spatial resolution of 1 mm of the NMR apparatus, the water content in this 1 mm zone could not be measured. At this moment, with respect to the one-dimensional spatial resolution, the NMR-technique is being developed further. As a continuation of the work presented in this paper, it is interesting to repeat the water extraction experiments with NMR thereby focussing on the interface zone between brick and mortar; in that case not only the moisture profile is measured in more detail but also the position of the interface and its displacement by compaction of the fresh mortar may be determined.
In cement mortars with air entraining agents, in the interface zone between brick and mortar, besides the water content also the carbonation of $Ca(OH)_2$ and its appearance seem different from

the middle of the mortar joint. This may be an important subject for further investigations for example with an electron microscope.

7. References

1. Brocken H.J.P., Moisture transport in brick masonry: the grey area between bricks Ph.D. thesis, Eindhoven University of Technology, The Netherlands (1998),
2. Sugo H.O., Page A.W. and Lawrence S.J., Influence of the macro & microstructure of air entrained mortars on masonry bond strength, Proc. 7th N. Am. Mas. Conf., 230-241 (1996).
3. Kopinga K. and Pel L., One-dimensional scanning of moisture in porous materials with nmr, *Rev. Sci. Instrum.* **65**, 3673-3681 (1994).
4. Brocken H.J.P., Spiekman M.E., Pel L., Kopinga K. and Larbi J.A., Water extraction out of mortar during brick laying: a NMR study, *Mater. Struct.* **31**, 49-57 (1998).
5. Bousfield B., Surface preparation and microscopy of materials, 1st ed. p. 291, Wiley, Chicester (1992).
6. American Society for Testing and Materials, astm Standard C457-95 "Standard Test Method for Microscopical Determination of Parameters of the Air-Void System in Hardened Concrete", 229-241 (1995).
7. French W.J., Concrete petrography: a review, *Quarterly Journal of Engineering Geology* **24**, 17-48 (1991).
8. Klug H.P. and Alexander L.E., X-Ray Diffraction Procedures, 2nd ed. p. 505, Wiley, New York (1974).
9. Brocken H.J.P., Pers N.M. van der and Larbi J.A., Composition of cement-lime and cement mortar as a function of distance to the brick-mortar interface: consequences for masonry, *submitted for publication in Mater. Struct.* (1999).
10. Neville A.M., Properties of concrete, 4th ed., Longman, London (1995).
11. Powers T.C., The properties of fresh concrete, Wiley, New York (1968).
12. Larbi J.A., Bijen J.M.J.M., Effects of water-cement ratio, quantity and fineness of sand on the evolution of lime in set portland cement systems, *Cem. Con. Res.* **20**, 783-794 (1990).